Conduction mechanism and shallow donor properties in silicon-doped -G a 2 O 3 thin films: An electron paramagnetic resonance study

H. von Bardeleben, Jean-Louis Cantin, A. Parisini, A. Bosio, R. Fornari

▶ **To cite this version:**

H. von Bardeleben, Jean-Louis Cantin, A. Parisini, A. Bosio, R. Fornari. Conduction mechanism and shallow donor properties in silicon-doped -G a 2 O 3 thin films: An electron paramagnetic resonance study. Physical Review Materials, 2019, 3 (8), pp.084601. 10.1103/PhysRevMaterials.3.084601 . hal-03924960

HAL Id: hal-03924960
https://hal.science/hal-03924960v1

Submitted on 20 Apr 2023

HAL is a multi-disciplinary open access archive for the deposit and dissemination of scientific research documents, whether they are published or not. The documents may come from teaching and research institutions in France or abroad, or from public or private research centers.

L'archive ouverte pluridisciplinaire **HAL**, est destinée au dépôt et à la diffusion de documents scientifiques de niveau recherche, publiés ou non, émanant des établissements d'enseignement et de recherche français ou étrangers, des laboratoires publics ou privés.

Conduction mechanism and shallow donor properties in silicon-doped ε-Ga_2O_3 thin films: An electron paramagnetic resonance study

H. J. von Bardeleben and J. L. Cantin
Sorbonne Université, Institut des NanoSciences de Paris 4, Place Jussieu, 75005 Paris, France

A. Parisini, A. Bosio, and R. Fornari
Department of Mathematical, Physical, and Computer Sciences, University of Parma, Viale delle Scienze 7/A, 43124 Parma, Italy

The defects in Si-doped ε-Ga_2O_3 epitaxial layers have been investigated by electron paramagnetic resonance (EPR) spectroscopy. The results show that Si doping introduces a single, paramagnetic defect, attributed to Si incorporation on the tetrahedral gallium lattice site. It is a spin $S = 1/2$ center with an axial g tensor with principal values of $g//c = 1.9573$ and $g\perp c = 1.9591$. The temperature dependence of the EPR parameter demonstrates that it is a shallow effective mass donor, which is at the origin of the n-type conductivity. The EPR spectrum is modified by motional narrowing effects, the analysis of which allows one to reveal different transport regimes, including localization, hopping conductivity, and ionization in the conduction band when the temperature is raised from $T = 4$ K to room temperature. Partial electrical compensation and donor clustering are equally evidenced by the EPR results, which are confirmed by correlated electrical transport measurements. Silicon is thus a promising dopant for the formation of highly conductive n-type ε-Ga_2O_3.

I. INTRODUCTION

Gallium oxide is a wide band-gap semiconductor, which can be grown in different polytypes α, β, γ, δ, and ε. Among them the β, α, and ε polytypes have recently attracted attention due to their interesting semiconducting properties, which allow promising applications in microelectronics [1]. The β polytype with its monoclinic crystal structure is the thermally most stable one and is available as single crystals [2] and in the form of epitaxial layers. The other two polytypes can be stabilized by epitaxial growth at specific lower growth temperatures [3–5]. For the growth of epitaxial layers c-plane sapphire has been found to be a convenient substrate due to a well-defined epitaxial relation.

The application of Ga_2O_3 in microelectronics requires suitable n-type and if possible p-type conductivity. n-type conduction is generally achieved by doping with shallow donors; however, most of the acceptors turn out to be deep and p-type conductivity at room temperature (RT) remains an unsolved issue in most transparent conducting oxide semiconductors. Unintentionally doped β-Ga_2O_3 bulk samples are often n-type conductive due to the presence of native, shallow donors, the nature of which has been discussed in several publications [6,7]. Whereas in early papers the shallow donor has been related to the presence of oxygen vacancy centers, this model is now discarded, as oxygen vacancies have been predicted to be deep donors [8]. The presently accepted model for the shallow donors in nonintentionally doped bulk β-Ga_2O_3 samples is the presence of a Si contamination. Whereas several group-IV dopants like Si, Ge, and Sn have been proposed for introducing n-type conductivity, according to recent calculations only Si on a tetrahedral Ga site can be expected to introduce a shallow donor level [9]. This has been experimentally confirmed for Si in the β polytype [7]. In the α polytype [10] Sn doping has been shown to be suitable for obtaining n-type conductivity. In both cases the group-IV dopants introduce shallow, effective mass donors with ionization energies in the 30-meV range [11]. The case of Sn in β-Ga_2O_3 is less established as Sn doping actually decreased the free concentration related to nonidentified native shallow donors [6].

Theory predicts Si in β-Ga_2O_3 to occupy preferentially tetrahedral Ga sites [8,9]. Further, according to these calculations among the possible donor dopants (C, Si, Sn, and Ge) only Si on a tetrahedral Ga site is expected to introduce a truly effective mass donor state with a predicted ionization energy of 36 meV [9]. One might expect that these predictions are also valid for ε-Ga_2O_3 due to its similar band structure. Whereas the α polytype contains only one type of Ga site, the lower symmetry of β and ε polytypes presents a more complex situation. In β-Ga_2O_3 we have two distinct Ga sites with distorted octahedral and tetrahedral symmetry, respectively. In ε-type Ga_2O_3 we have three distinct Ga sites (Fig. 1), two of which have a distorted octahedral symmetry (Ga_1 and Ga_2 in Fig. 1) and one of which has a distorted tetrahedral symmetry (Ga_3 in Fig. 1), organized in a 4H stacked structure [4,5]. In ε-Ga_2O_3, layers containing only octahedral sites (Ga_1) occupied by Ga atoms in a 2/3 ratio are alternated with layers where Ga atoms occupy both octahedral (Ga_2) and tetrahedral (Ga_3) sites. Thus, Si doping raises the issues of on which lattice sites the dopant is incorporated and what are the related electronic properties. For 3d transition metals in β-Ga_2O_3 it has been shown previously by EPR that they occupy both octahedral and tetrahedral Ga lattice sites at comparable concentrations. The different point symmetry

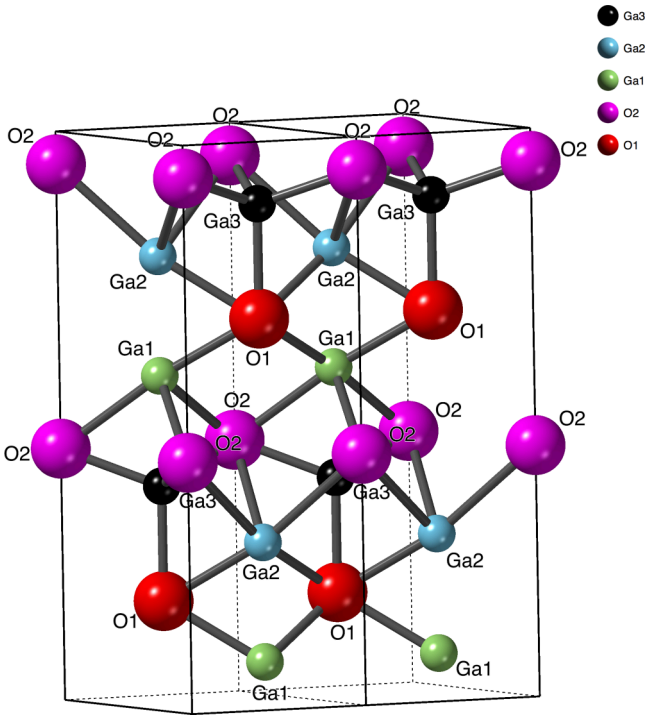

FIG. 1. ε-Ga_2O_3 structure representation. The structure contains three nonequivalent Ga sites—two distorted octahedral Ga sites (Ga_1, Ga_2) and one distorted tetrahedral Ga site (Ga_3)—and two nonequivalent oxygen sites (O_1, O_2). Please note, that the two octahedral $Ga_{1,2}$ sites are different from the crystallographic point of view [5], but when occupied by donor impurities, they give rise to equivalent donor states.

leads to different spin Hamiltonian parameters, which allows, for example, $Fe_{oct}{}^{3+}$ and $Fe_{tetra}{}^{3+}$ to be easily distinguished in spite of their identical ^6S ground state [12]. In addition to the paramagnetic properties, the electronic properties of Fe, a deep acceptor in β-Ga_2O_3, might equally depend on the lattice site. In previous deep level transient spectroscopy studies a $(-/0)$ charge transition level at $E_c = 0.7\,\text{eV}$ has been associated with Fe doping [13], but the question of which of the two centers Fe_{octa} or Fe_{tetra}, is related to this level has not yet been clarified. In the case of the α polytype with the hexagonal crystal structure, Ga site substituted Sn has been shown to be a highly soluble dopant introducing a shallow donor level [10].

In this paper we focus on Si doping of ε-Ga_2O_3 thin films and the analysis of the donor/defect properties and their incorporation on the different lattice sites. We applied electron paramagnetic resonance (EPR) spectroscopy for the investigation of the magnetic and electronic properties of highly Si-doped ε-polytype heteroepitaxial layers. The EPR technique is known to be well suited for the study of deep and shallow donors in their paramagnetic neutral charge state as it allows the determination of the main spin Hamiltonian parameters, such as the electron spin S, the g tensor, the point symmetry, and a quantitative determination of the defect concentration. But its utility for determining transport processes has not yet been sufficiently recognized. In case of structural imperfections of thin films, such as twins or

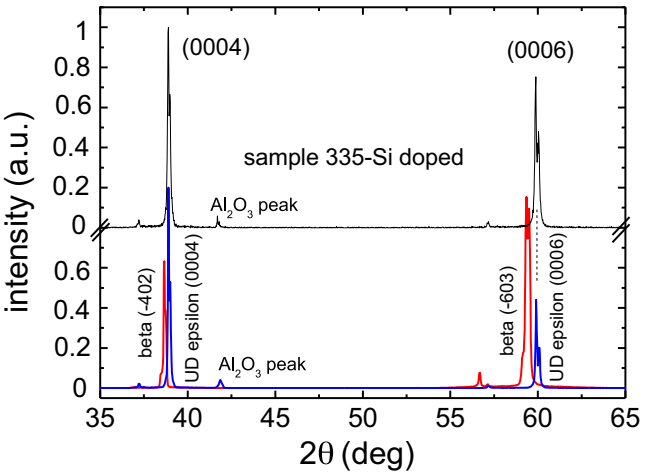

FIG. 2. X-ray-diffraction pattern of the Si-doped ε-Ga_2O_3 epitaxial layer (black) and the comparison with an undoped sample (blue) and a β-Ga_2O_3 substrate (red).

a multiple grain structure, the EPR technique is also useful for structural analysis as such imperfections will give rise to a multiplicity of the EPR spectra. In this paper we demonstrate, in particular, that the temperature dependence of the EPR parameters contains useful information of the dynamic properties of the donor electrons and thus on the transport properties which are normally deduced only from electrical measurements.

II. EXPERIMENTAL DETAILS

The ε-epitaxial layers have been grown by metal-organic chemical vapor deposition (MOCVD) at 60 mbars on c-plane sapphire substrates heated at 600–610 °C. Trimethylgallium and ultrapure water were used as precursors with partial pressures of the reagents in the growth chamber ($pH_2O/pTMG$) in a ratio of about 150. As carrier gas, ultrapure H_2 was used, with a flow of 2000 sccm. The layers were Si doped by adding silane in the gas phase during the growth process. Time-of-flight secondary ion mass spectroscopy (TOF-SIMS) measurements confirmed the incorporation of silicon into the film [14]. Typical layer thickness was 0.5 μm. The ε phase of the layers was verified by x-ray-diffraction measurements [15]. The x ray also showed that the films maintained the same c orientation of the sapphire substrate. Figure 2 shows the Cu Kα radiation x-ray-diffraction pattern of a sample studied in this paper. Note the perfect correspondence with the (0004) and (0006) peaks of an undoped reference ε-Ga_2O_3 layer (we used the four-index notation valid for the pseudohexagonal ε crystallographic structure). Note also the splitting of the peaks of both undoped and Si-doped films, due to Kα1 and Kα2 radiations of the utilized anode, which indicates a very good crystallographic quality. In addition, we determined the in-plane orientation of the films: the directions $[10\bar{1}0]$ and $[\bar{1}2\bar{1}0]$ were at about 6.8° from the sides of the rectangular samples. We made use of the four-index notation considering the pseudohexagonal structure of the ε-Ga_2O_3 lattice [4], although it is definitely known that this polymorph is orthorhombic at the microscopic level [5]. However, as explained in [4,5], when low resolution experimental techniques are applied, such as

EPR and resistivity measurements, a more practical hexagonal notation can be used.

The electrical properties of the samples have been investigated in the temperature range 17.5 to 300 K. We used a standard van der Pauw configuration with Ti/Au double layer contacts deposited by sputtering on the corners of 5×5-mm^2 square-shaped samples [14]. The RT resistivity of the sample investigated here was 0.47 Ω cm and the Hall density was 2.9×10^{18} cm^{-3}. In the case of hopping conductivity, which is the case here as shown below, the carrier concentration is weakly temperature dependent and comparable to the net donor density. The electrical transport measurements have been reported before [14] but will be reproduced here for comparison with the EPR measurements.

For the EPR studies we used samples of size 6×4 mm^2 cut from the same substrate. The EPR measurements have been performed with an x-band spectrometer (9 GHz) under standard conditions: 100-kHz magnetic field modulation and lock-in detection. The samples were investigated in the temperature range from $T = 4$ K to room temperature. The spin Hamiltonian parameters were obtained from the angular variation of the EPR spectra for a rotation of the applied magnetic field in three lattice planes. The line shape and linewidth were determined by simulation with Gaussian and Lorentzian line shapes. These line shapes are the ones expected for localized and delocalized donors, respectively. The intensity of the EPR signal was obtained by a double integration.

The absolute spin concentration (spins/cm^3) was determined at room temperature by the simultaneous measurement of the Ga_2O_3 film and a spin standard sample (Al_2O_3 : Cr) containing 9.2×10^{15} spins; the standard sample was obtained from the National Bureau of Standards. The spin concentrations were obtained by a double integration of the respective EPR spectra, corrected for the different spin values of $S = 1/2$ (Si donor) and $S = 3/2$ (Cr^{3+} center in the standard sample), respectively.

III. RESULTS AND DISCUSSIONS

A. EPR results

While no EPR spectrum is observed in undoped samples, the Si-doped samples present an anisotropic single line spectrum observable already at room temperature. In Fig. 3 we show representative EPR spectra of a highly doped sample (no. 335), which allows an EPR analysis in the whole temperature range from 4 to 300 K. A single line spectrum is the fingerprint of a spin $S = 1/2$ center, such as expected for a neutral donor with two ionization states (0/+). The EPR spectra are characterized by a Lorentzian line shape and a surprisingly small peak-to-peak linewidth of only $\Delta Bpp = 1.0$ G. In principle, we would expect for a localized defect in Ga_2O_3 a much larger linewidth (>10 G) due to the super-hyperfine (SHF) interaction with the neighboring Ga nuclei, all of which have a nuclear spin of $I = 3/2$. In addition, the SHF interaction should give rise to a Gaussian line shape due to inhomogeneous broadening effects. The observations of a reduced linewidth and a Lorentzian shape are indications of a delocalization of the donor electron with a modification of the EPR spectra by a motional narrowing effect. As shown below, this is confirmed by the temperature dependence of

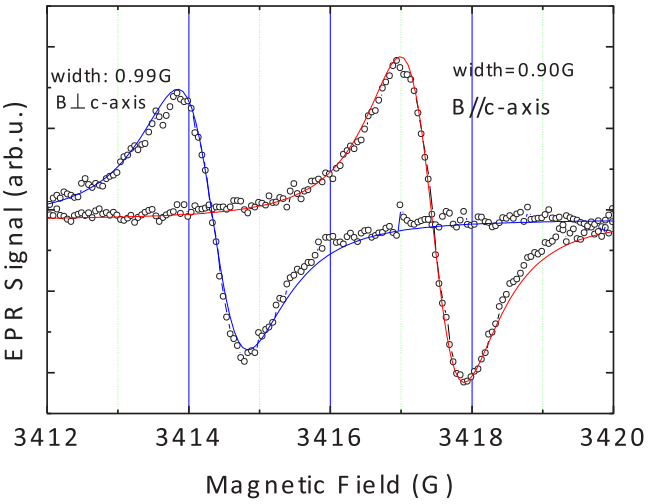

FIG. 3. Room-temperature EPR spectrum (circle) for the $B//c$ axis (red) and $B\perp c$ axis (blue); the spectra are characterized by a Lorentzian line shape (red line) and linewidth of $\Delta Bpp = 0.90$ and 0.99 G, respectively.

the EPR spectra. The delocalization of the donor electrons depends on the donor concentration and on the Bohr radius of the donor wave function; delocalization and impurity band formation are generally estimated by the Mott criterion, which predicts a metal-insulator transition for $N^{1/3}a_B = 0.27$, with N the donor concentration and a_B the donor Bohr radius. In β-Ga_2O_3 the Bohr radius was reported as $a_B = 1.8$ nm and impurity band formation is thus expected for a donor concentration of $N = 4 \times 10^{18}$ cm^{-3}. In the case of Sn-doped α-Ga_2O_3, impurity band formation has been shown to occur for a donor concentration of 4×10^{18} cm^{-3} [10].

We determined with EPR the concentration of the $S = 1/2$ center in this Si-doped ε-Ga_2O_3 film by a simultaneous measurement with the spin standard sample. We obtained a value of 2.3×10^{13} spins, which corresponds to an average concentration of 2.1×10^{18}-cm^{-3} spins, assuming a homogeneous distribution of the defect over the whole sample thickness. This assumption has been confirmed by TOF-SIMS measurements, which have shown the homogeneity of the Si incorporation [14]. The Hall effect measurements at RT of the same sample indicated a carrier concentration of $n = 2.9 \times 10^{18}$ cm^{-3}. Within the uncertainties of each method of investigation, these values are in good agreement and we can conclude that the paramagnetic defect is directly related to the n-type conductivity.

The principal values and axes of the g tensor of the donor were determined by the measurements of the resonance fields in three orthogonal lattice planes (Fig. 4). For a rotation of the magnetic field in the film plane we observed an isotropic g factor; the g tensor is thus axial with the principal axis parallel to the crystal c axis. Its principal values at $T = 300$ K are $g = 1.9573$ for $B//c$ and $g = 1.9591$ for $B\perp c$. These values are only marginally temperature dependent. The small variation is attributed to the gradual change from conduction electron-spin resonance to shallow donor resonance when the temperature is lowered from RT. The isotropic character of the g tensor in the film plane might be at first surprising as the point symmetry on both lattice sites is lower than axial. However,

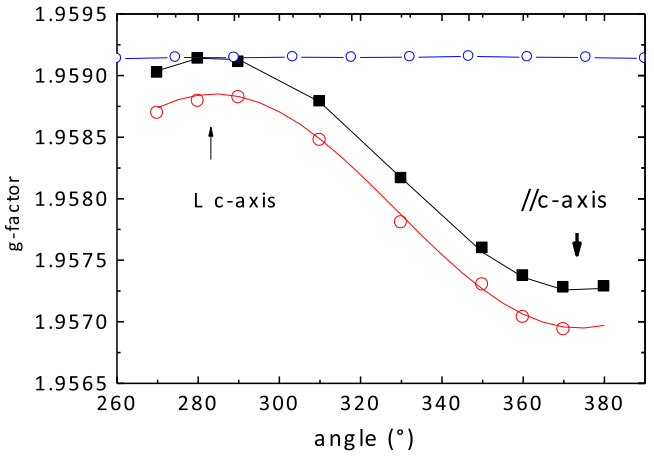

FIG. 4. Angular variation of the effective g factor for a rotation of the magnetic field from $B//c$ to $B\perp c$. $T = 300$ K (black) and $T = 4$ K (red); angular variation around the c axis (blue) is at $T = 300$ K.

as shown below, the delocalization of the donor wave function and the hopping conduction is expected to average out a small in-plane anisotropy. At room temperature, when we observe conduction electron-spin resonance, only the conduction-band (CB) anisotropy will be relevant for the determination of the g tensor anisotropy.

The EPR linewidth and the EPR signal intensity both show a strong dependence on the measurement temperature with three different temperature regimes, $4 < T < 50$, $50 < T < 100$, and $T > 100$ K. When we lower the temperature from $T = 295$ to 4 K, we observe an increase of the linewidth [Figs. 5 and 6(a)], a change in intensity of the EPR spectrum [Fig. 6(b)], and a small shift of the g values [Fig. 6(c)]. These variations are not monotonic but occur in specific temperature regions, which correspond to different electrical transport regimes.

The variation of the g factor with temperature is small but is nevertheless resolved due to the small linewidth of the spectra in the temperature region $T = 295$ to 50 K. For

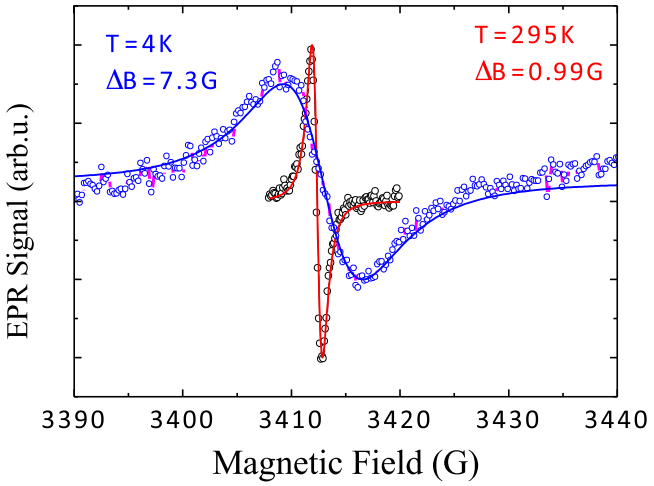

FIG. 5. EPR spectra for $T = 295$ K (circle, red) and $T = 4$ K (diamond, blue); the lines are fit with Lorentzian line shapes (line) for the $B//c$ axis.

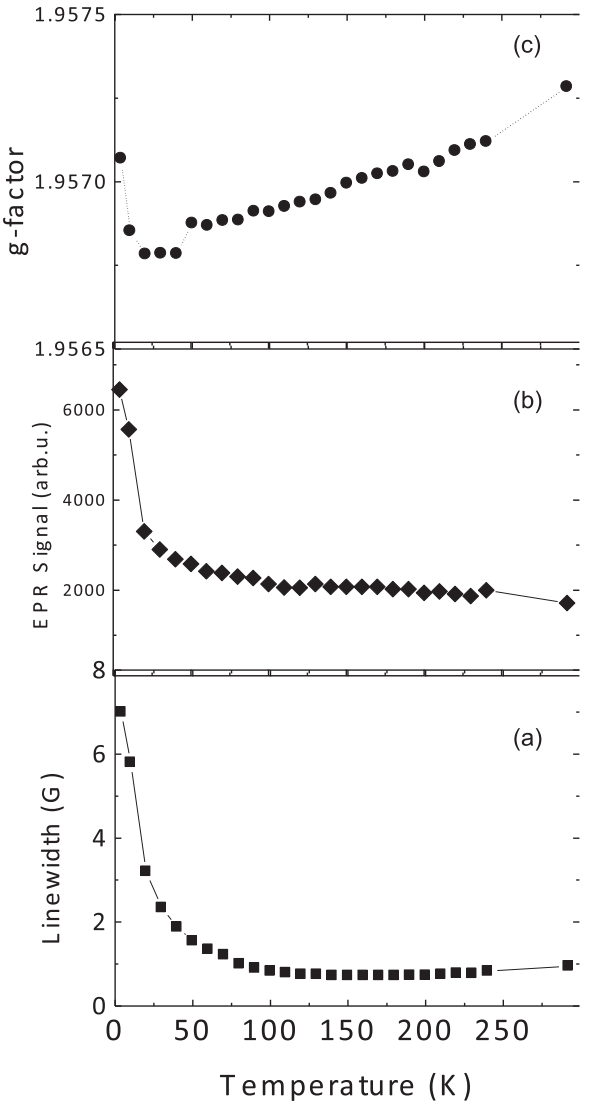

FIG. 6. (a) Temperature dependence of the EPR linewidth ΔB_{pp} between room temperature and $T = 4$ K for the $B//c$ axis. (b) Temperature dependence of the EPR signal intensity obtained by double integration of the experimental spectrum. (c)Temperature dependence of the effective g factor for $B//c$.

the principal value $g//c$ the shift is $\Delta g = 0.0005$ [Fig. 6(c)]. At the lowest temperature of $T = 4$ K the g value increases slightly again. Note however that in this low-temperature (LT) range the linewidth increases strongly and thus the error in the resonance field determination is also increased. The small variation is attributed to the gradual change from conduction electron-spin resonance to shallow donor resonance when the temperature is lowered from RT. The g values for conduction electrons and shallow effective mass donors are expected to be very similar as both are derived from the CB structure. Thus the observation of nearly identical g values in the whole temperature range is an indication that the paramagnetic donor observed Si is effective masslike.

The temperature dependence of the EPR signal intensity [Fig. 6(b)] is rather unusual but similar to those observed previously for the shallow donors in highly doped α-Ga_2O_3 [10]

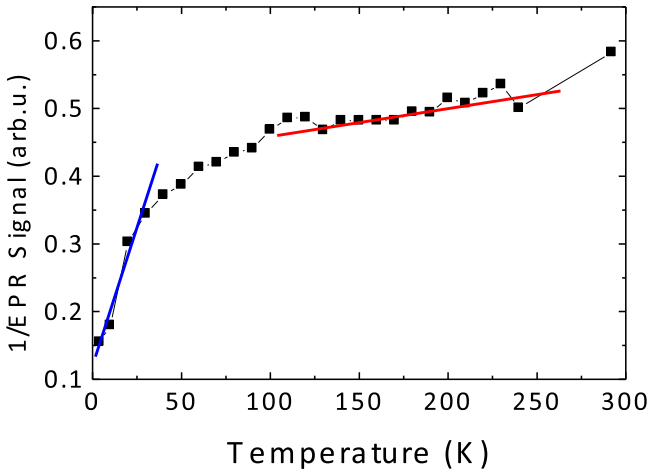

FIG. 7. Inverse of the EPR signal intensity vs temperature.

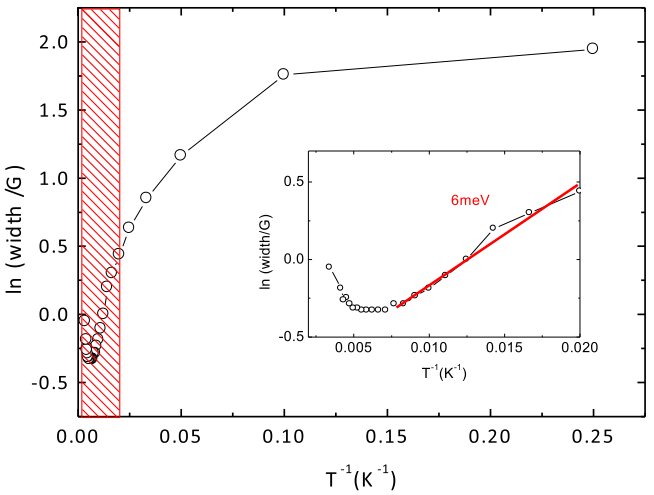

FIG. 8. EPR linewidth (dot) $\ln(\Delta B_{pp})$ vs T^{-1}, and simulation (inset, red lines) of the high-temperature part with an Arrhenius law.

and β-Ga_2O_3 [7,8]. As seen in Figs. 6(b) and 7 we observe a nearly constant EPR signal intensity between $T = 295$ and 100 K, and a strong increase for $T < 50$ K. A temperature-independent susceptibility is the characteristic of conduction electron resonance (Pauli susceptibility), whereas for localized donor electrons a Curie-type paramagnetism, with an EPR signal intensity variation $I \sim 1/T$, should be observed. The case of delocalized donor states with impurity band formation presents an intermediate situation. In principle, both neutral donors and the conduction electrons can be observed by EPR spectroscopy and close to the ionization temperature of the donors both of them will be detected simultaneously. As the g tensors of effective mass donors and conduction electrons are generally very similar their EPR spectra are often indistinguishable [16]. The most direct distinction between the two systems is given by their different susceptibilities. The Pauli-like susceptibility, which we observe for $T > 100$ K, shows that in this temperature range the donors are ionized and the electrons are moving in the conduction band. On the contrary for $T < 50$ K the electrons are localized on the donors.

Additional information on the donor properties is obtained from an analysis of the EPR linewidth. The observed temperature dependence of the linewidth is consistent with the model of variable range hopping (VRH) conductivity [17–19]. VRH will modify the EPR linewidth by motional narrowing, if the hopping frequency ν is high enough, such that the condition $\nu > \gamma_{\Delta B}$ is fulfilled [20]. γ_e is the electron magnetogyric ratio and ΔB is the half width at half-height width of the absorption line, which is related to the peak-to-peak width of the experimentally observed first derivative line shape ΔB_{pp} by $\Delta B_{pp} = 2/3^{0.5}\ \Delta B$. In our case with a typical linewidth of 10 G, this corresponds to a hopping frequency of $\nu \geqslant 1 \times 10^7$ s^{-1}. In many cases this process is thermally activated. To determine the corresponding activation energy E_a we have plotted the temperature dependence of the linewidth in an Arrhenius plot (Fig. 8):

$$\Delta B_{pp}(T) = \Delta B_0 e^{-E_a/k_B T} \qquad (1)$$

with ΔB_0 a constant, E_a the activation energy, and k_B the Boltzmann constant.

We observe a linear variation of $1/T$ between 0.008 and 0.020 (inset of Fig. 8), from which we deduce an activation energy of 6 meV. For higher temperatures ($T > 150$ K) we can no longer analyze the linewidth as we approach the intrinsic, homogenous linewidth of the donor EPR spectrum, which cannot be further reduced by the motional narrowing. It should be noted that a very similar activation energy of $E_A = 7$ meV has been observed for Sn shallow donors in Sn-doped α-Ga_2O_3 epitaxial layers with comparable room-temperature conductivity and doping level Sn $= 4.6 \times 10^{18}$ cm^{-3} [10]. This similarity suggests attributing in both cases the activation energy to the first excited state of an effective mass donor; in this model, also the ionization energy of the Si donor in ε-Ga_2O_3 can be expected to be similar to that one of the Sn donor in the α polytype [10], an established shallow donor in α-Ga_2O_3. Self-consistently, the very similar g tensor indicates also a comparable electron effective mass of $\sim$0.3 m_e for the conduction-band minimum at the Γ point of the Brillouin zone in the two Ga_2O_3 polytypes, m_e being the bare electron mass [21,22]. Moreover, because in ε-Ga_2O_3 the g tensor anisotropy is small, $\Delta g = 0.0018$, the effective mass anisotropy is equally expected to be weak. As the neutral donor concentration in these samples is only close to the critical Mott value of 2.5×10^{18} cm^{-3}, assuming a dielectric constant and an effective mass comparable to those of the beta polytype, these results might indicate a donor clustering by which the local electron density can approach the Mott value. Thus, we give here an approximate evaluation of a band parameter for the ε polytype of Ga_2O_3.

Further insight into the conduction mechanism is obtained from the analysis of the linewidth ΔB_{pp} at low temperature (Fig. 9). The small and temperature-independent linewidth in the range from $T = 295$ to 100 K is coherent with the model of conduction electron-spin resonance, where due to motional narrowing the intrinsic linewidth of the conduction electrons will be observed. At lower temperatures impurity band conduction becomes dominant and the linewidth ultimately depends on the hopping frequency. Generally, VRH conduction is observed in disordered materials such as amorphous a-C

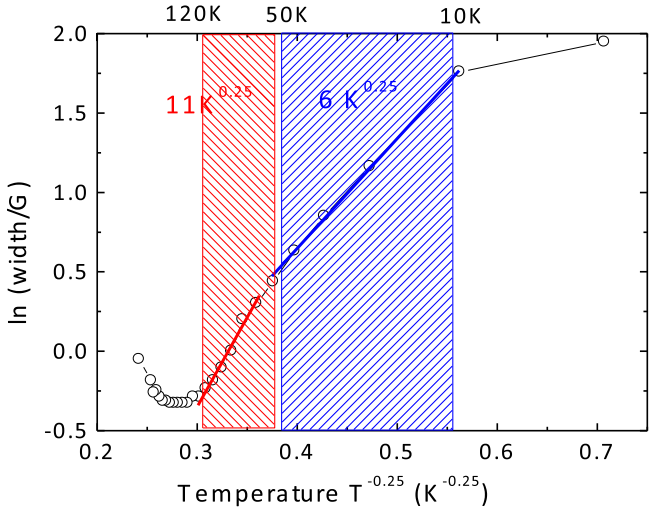

FIG. 9. EPR linewidth $\ln(\Delta B_{pp})$ vs $T^{-0.25}$ (circle), and simulation (red, blue lines) corresponding to a 3D VRH hopping processes in two temperature regions.

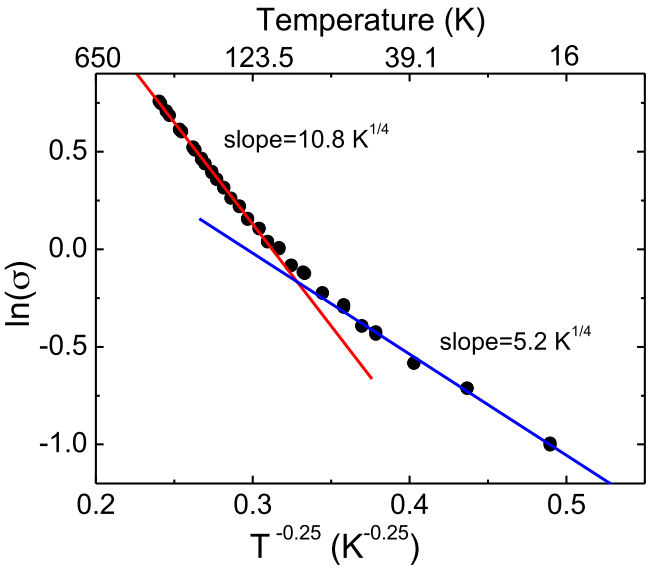

FIG. 10. Logarithm of the conductivity (in Ω^{-1} cm^{-1}) vs $T^{-1/4}$. Lines: Linear fits of the data at high (red) and low (blue) temperatures. The estimated slopes are ${T_0}^{0.25} = (10.8 \pm 0.1)$ K$^{0.25}$ in the 50- to 100-K temperature range and ${T_0}^{0.25} = (5.2 \pm 0.2)$ K$^{0.25}$ in the range 50 to 10 K.

and a-Si and highly doped semiconductors [17,18,23]. Nevertheless in our case the observation of VRH is not unexpected, given the partial compensation of the donors, the random distribution of the D^0 and D^+ donor states, and the crystal structure with partial occupation of tetrahedral Ga_3 sites. As shown below, the VRH is directly confirmed by the transport measurements. We have thus analyzed the linewidth variation in the temperature range below ionization in this model:

$$\Delta B_{pp} = \Delta B_\infty \exp\left[-\left(\frac{T_0}{T}\right)^{1/4}\right]. \qquad (2)$$

We have fitted the linewidth variation by Eq. ((2) The fit (Fig. 9) shows indeed a linear variation in agreement with the model of VRH. We observe however two distinct temperature regions: a first one with a slope of ${T_0}^{0.25} = (11 \pm 1)$ K$^{0.25}$ in the 50- to 100-K temperature range and a second one with a slope of ${T_0}^{0.25} = (6 \pm 1)$ K$^{0.25}$ in the range 50 to 10 K, the meaning of which will be discussed in view of the transport data reported below.

B. Hall measurement results

The conductivity (Fig. 10) exhibits the typical temperature dependence of variable range hopping transport, with two distinct temperature regions, as also observed by the EPR measurements. The expression for three-dimensional (3D) VRH conductivity is [17,18,24]

$$\sigma = \sigma_\infty \exp\left[-\left(\frac{T_0}{T}\right)^{1/4}\right] \qquad (3)$$

with σ_∞ a prefactor and T_0 a material specific parameter. We observe two different temperature regions, where the slope of the Mott plots shows a linear behavior: a slope of ${T_0}^{0.25} = (10.8 \pm 0.1)$ K$^{0.25}$ in the 50- to 100-K temperature range and a slope of ${T_0}^{0.25} = (5.2 \pm 0.2)$ K$^{0.25}$ in the range 50 to 10 K. These regions correspond to two different transport processes.

The low-temperature data (Figs. 9 and 10) show an excellent agreement between electrical and EPR data. As at LT the EPR spectra indicate electrons localized on shallow donors, we can suppose that such a LT-VRH mechanism is due to a hopping conduction through individual Si donors on tetrahedral Ga sites (Ga_3 sites in Fig. 1). From the localization length ξ, expected to be a few nanometers [14], information on the density of localized sites involved in the hopping transport, $N_S(T)$, can be derived. In fact, in the Mott theory, $T_0 = C/[\xi^3 g(\mu) K_B]$, where $C = 8^3/9\pi \approx 18.1$ for a 3D noninteracting electron gas and randomly distributed hopping sites, K_B is the Boltzmann constant, whereas $g(\mu)$ is the density of the localized energy states lying in proximity of the Fermi level and within an energy bandwidth $\omega_{\rm opt} = 0.25 K_B T (T/T_0)^{1/4}$ (optimal energy), so that from the LT slope of the data $g(\mu)$ can be obtained and then $N_S(T) = g(\mu)\omega_{\rm opt}$ [24]. Its value is close to 10^{19} cm^{-3} at $T = 25$ K; it is consistent with both the net donor density measured by EPR and the measured RT Hall density [14]. A prerequisite for VRH is the presence of ionized donors and thus the presence of compensating acceptors in comparable concentration; in our case an acceptor density of $N_A > 10^{17}$ cm^{-3} can be estimated. As acceptors were not introduced purposely by doping, they must be of native character, either intrinsic or impurity related. Probable intrinsic acceptors are Ga vacancies, which are known to be deep acceptors in β-Ga_2O_3 [26]. In n-type conducting thin films they are in a diamagnetic charge state [25–27], and will not be detectable by EPR. Often, Fe contamination can be another source of electrical compensation in Ga_2O_3. Even though paramagnetic in the negatively charged acceptor state, the sensitivity of the EPR technique is insufficient to detect them in thin films as investigated here for concentrations below 10^{18} cm^{-3}.

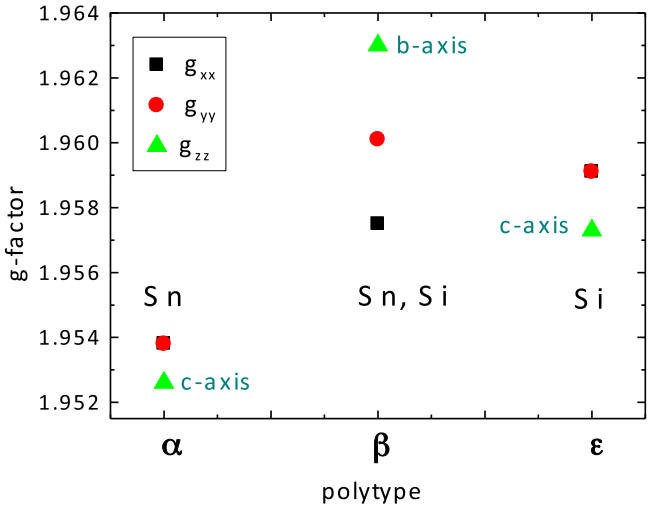

FIG. 11. Principal values and axes of the g tensor of shallow donors in three Ga_2O_3 polytypes: Si and Sn donors in the β polytype, Si donor in the ε polytype, and Sn donor in the α polytype.

To explain the existence of two low-temperature regimes we consider the model of dopant clustering. The theory of heavily doped semiconductors predicts that indeed dopant clusters of different size can form [28,29], depending on the doping level up to the metal to insulator transition. These phenomena have been studied in detail by different techniques, such as transport, optical, and magnetic resonance experiments, in the case of phosphorous-doped silicon [29]. At low temperatures, electrons in clusters do not contribute significantly to the macroscopic dc conductivity [29]. However, the onset of a thermally activated conductivity between cluster states, which has the features of the VRH conduction, may become possible, as predicted by the percolation theory [28]. It is also important to note that the observed high-temperature (HT) HT-VRH behavior is related to the doping level, as it shows a doping-dependent slope of the $\ln\sigma$ data plotted vs $T^{-1/4}$ [13]. Hopping between donor clusters has been not yet been reported in other Ga_2O_3 polymorphs with comparable doping level. In ε-Ga_2O_3 such a situation could be favored by a nonrandom dopant distribution, induced by the oxygen-plane 4H stacking and the distribution of tetrahedral Ga_3 sites within planes orthogonal to the c axis, separated by planes containing only octahedral Ga sites (Ga_1).

The results of our combined EPR and Hall measurements lead thus to the following model for the Si donor in ε-Ga_2O_3.

(i) Si doping introduces one paramagnetic defect, which has the properties of a shallow effective mass donor; this property combined with the theoretical predictions of [9] allows us to attribute this center to Si on a tetrahedral Ga_1 lattice site. The incorporation of Si on the octahedral Ga_2 and Ga_3 sites seems to be negligible, as no second Si related paramagnetic defect is observed.

(ii) The observed axial symmetry of the g tensor is at first sight surprising as the point symmetry of the Si donor on a distorted tetrahedral Ga_3 site is orthorhombic. However, the combined effect of the ε layers not being perfectly single crystalline but composed of nanometer sized orthogonal κ domains separated by 120° twins and the effective mass character of the donor do not allow one to detect a potential in-plane anisotropy.

(iii) The principal values of the g tensor ($\approx$1.95) are typical for shallow donors in the α and β polytypes and also for donors in transparent conductive oxides such as ZnO [30] (Fig. 11). All of them are shallow donors with ionization energies in the range of $\sim$30 meV [6,7,9,10]. Thus, Si is the preferred shallow donor to grow n-type conductive thin films similar to the case of Si in the β polytype.

(iv) The films are partially electrically compensated by the presence of unidentified acceptors. The conductivity is dominated by variable range hopping between Si donor sites with a nonrandom donor distribution.

IV. CONCLUSION

Doping of ε-Ga_2O_3 epitaxial layers by silane introduces a shallow effective mass donor, which we attribute to Si substituted on tetrahedral Ga_3 sites. Its solubility is high as free-carrier concentrations of 2.1×10^{18} cm^{-3} were obtained by this doping procedure. At room temperature the donor electrons are delocalized and the EPR spectra are modified by motional narrowing effects with hopping frequencies $>10^7$ s^{-1} in the low-temperature region. At temperatures below $T < 100$ K conduction takes place via VRH hopping. The observation of VRH demonstrates a partial compensation of the donors by native acceptors. Ga vacancies, which are thought to behave as deep acceptors, or Fe contamination may be the source of these compensating centers; however, the origin of the acceptors could not be established in this paper. Finally, we wish to underline the very good agreement between the results of electrical transport measurements and contact-free EPR measurements, which corroborates the interpretation of the transport model and confirms the potential of EPR spectroscopy to study conduction processes.

ACKNOWLEDGMENTS

The authors wish to thank Dr. Matteo Bosi of IMEM-CNR; Dr. Vincenzo Montedoro and Sig. Salvatore Vantaggio of Department of Mathematical, Physical, and Computer Sciences, University of Parma (SMFI-UniPR), for their contribution in the growth and processing of the samples; Dr. Sara Beretta of IMEM-CNR for x-ray-diffraction measurements and sample orientation; and Prof. Giuseppe Allodi of Department SMFI-UniPR for useful discussions.

[1] S. J. Pearton, J. Yang, P. H. Cary IV, F. Ren, J. Kim, M. J. Tadjer, and M. L. A. Mastro, Appl. Phys. Rev. **5**, 011301 (2018).

[2] A. Kuramata, K. Koshi, S. Watanabe, Yu Yamaoka, T. Masui, and S. Yamakoshi, Jpn. J. Appl. Phys. **155**, 1202A2 (2016).

[3] D. Shinohara and S. Fujita, Jpn. J. Appl. Phys. **47**, 7311 (2008).

[4] F. Mezzadri, G. Calestani, F. Boschi, D. Delmonte, M. Bosi, and R. Fornari, Inorganic Chemistry **55**, 12079 (2016).

[5] I. Cora, F. Mezzadri, F. Boschi, M. Bosi, M. Čaplovičová, G. Calestani, I. Dódony, B. Pécz, and R. Fornari, Cryst. Eng. Comm. **19**, 1509 (2017).

[6] M. Yamaga, E. G. Víllora, K. Shimamura, N. Ichinose, and M. Honda, Phys. Rev. B **68**, 155207 (2003).

[7] N. T. Son, K. Goto, K. Nomura, Q. T. Thieu, R. Togashi, H. Murakami, Y. Kumagai, A. Kuramata, M. Higashiwaki, A. Koukitu, B. Monemar, and E. Janzén, J. Appl. Phys. **120**, 235703 (2016).

[8] J. B. Varley, J. R. Weber, A. Janotti, and C. G. Van de Walle, Appl. Phys. Lett. **97**, 142106 (2010).

[9] S. Lany, APL Materials **6**, 046103 (2018).

[10] E. Chikoidze, H. J. von Bardeleben, K. Akaiwa, E. Shigematsu, K. Kaneko, S. Fujita, and Y. Dumont, J. Appl. Phys. **120**, 025109 (2016).

[11] E. G. Víllora, K. Shimamura, Y. Yoshikawa, T. Ujiie, and K. Aoki, Appl. Phys. Lett. **92**, 202118 (2008).

[12] R. Buescher, Z. Naturforsch **42a**, 67 (1987).

[13] M. E. Ingebrigtsen, J. B. Varley, A. Yu. Kuznetsov, B. G. Svensson, G. Alfieri, A. Mihaila, U. Badstübner, and L. Vines, Appl. Phys. Lett. **112**, 042104 (2018).

[14] A. Parisini, A. Bosio, V. Montedoro, A. Gorreri, A. Lamperti, M. Bosi, G. Garulli, S. Vantaggio, and R. Fornari, APL Materials **7**, 031114 (2019).

[15] F. Boschi, M. Bosi, T. Berzina, E. Buffagni, C. Ferrari, and R. Fornari, J. Cryst. Growth **443**, 25 (2016).

[16] D. V. Savchenko, E. N. Kalabukhova, A. Pöppl, E. N. Mokhov, and B. D. Shanina, Phys. Status Solidi B **248**, 2950 (2011).

[17] N. F. Mott, Philos. Mag. **19**, 835 (1969).

[18] C. Godet and J. P. Kleider, J. Mater. Sci.: Mater. Electron. **17**, 413 (2006).

[19] A. Parisini, A. Parisini, and R. Nipoti, J. Phys.: Condens. Matter **29**, 035703 (2017).

[20] A. Abragam, *The Principles of Nuclear Magnetism* (Clarendon, Oxford, 1961).

[21] H. He, R. Orlando, M. A. Blanco, R. Pandey, E. Amzallag, I. Baraille, and M. Rérat, Phys. Rev. B **74**, 195123 (2006).

[22] Z. Guo, A. Verma, X. Wu, F. Sun, A. Hickman, T. Masui, A. Kuramata, M. Higashiwaki, D. Jena, and T. Luo, Appl. Phys. Lett. **106**, 111909 (2015).

[23] W. C. Mitchel, A. O. Evwaraye, S. R. Smith, and M. D. Roth, J. Electron Mater **26**, 113 (1997).

[24] B. I. Shklovskii and A. L. Efros, *Electronic Properties of Doped Semiconductors* (Springer-Verlag, Berlin, 1984), Vol. 45.

[25] B. E. Kananen, L. E. Halliburton, K. T. Stevens, G. K. Foundos, and N. C. Giles, Appl. Phys. Lett. **110**, 202104 (2017).

[26] H. J von Bardeleben, S. Zhou, U. Gerstmann, D. Skachkov, W. R. L. Lambrecht, Q. D. Ho, and P. Deák, APL Materials **7**, 022521 (2019).

[27] D. Skachkov, W. R. L. Lambrecht, H. J. von Bardeleben, U. Gerstmann, Quoc Duy Ho, and P. Deák, J. Appl. Phys. **125**, 185701 (2019).

[28] R. Riklund and K. A. Chao, Phys. Rev. B **26**, 2168 (1982).

[29] P. P. Altermatt, A. Schenk, and G. Heiser, J. Appl. Phys. **100**, 113714 (2006).

[30] J. E. Stehr, B. K. Meyer, and D. M. Hofmann, Appl. Mag. Reson. **39**, 137 (2010).